

## Recent Variations of Atmospheric Turbidity at Selected Sites in Finland, Estonia and Norway as Revealed by Surface Solar Radiation Measurements

Heikinheimo, M.J.<sup>1</sup>, H. Ohvri<sup>2</sup>, A. Venäläinen<sup>1</sup>, A. Skartveit<sup>3</sup>,  
J.A. Olseth<sup>3,4</sup>, V. Laine<sup>1</sup>, H. Teral<sup>2</sup>, M. Arak<sup>2</sup> and K. Teral<sup>2</sup>

<sup>1</sup>Finnish Meteorological Institute, P.O. Box 503, FIN-00101 Helsinki, Finland

<sup>2</sup>University of Tartu, Department of Environmental Physics, Ülikooli 18, Tartu, EE2400 Estonia

<sup>3</sup>University of Bergen, Geophysical Institute, Allegaten 70, 5007 Bergen, Norway

<sup>4</sup>Also affiliated to the Norwegian Meteorological Institute

(Received: December 1995; Accepted: August 1996)

### Abstract

Recent mean changes in atmospheric turbidity, expressed as the total aerosol transmittance  $\tau_a$  and as an atmospheric integral transparency coefficient AITC, were analysed using routine surface solar irradiance measurements from selected sites: Jokioinen, Jyväskylä and Sodankylä in Finland, Tiirikoja in Estonia and Bergen in Norway. At all sites, except Bergen, the turbidity for the three summer months analysed generally increased (transmittance or AITC decreased) from the 1960's to the 1970's, whereas for the period from 1971 to 1991, the corresponding trends for AITC and aerosol transparency were somewhat uncertain due to an overlap with temporary minima in transparency caused by the volcanic eruptions of El Chichon and Mt. Pinatubo. These minima could be well identified in the time series, having a relative anomaly in the aerosol optical thickness close to 0.10 and 0.25, respectively. The mean increase in turbidity preceding the Mt. Pinatubo eruption was estimated to contribute to some 0.4% reduction on mean global irradiance from the 1960's to the 1980's.

*Key words:* aerosol transmittance, atmospheric transparency, turbidity, solar radiation

### 1. Introduction

At many locations long-term monitoring of the surface solar irradiance has revealed significant increases in atmospheric turbidity, particularly in the northern hemisphere industrialised regions (e.g. Ball and Robinson, 1982; Russak, 1990), but increases have also been notable in the records of the Arctic (McGuffie *et al.* 1985; Radionov and Marshunova, 1992). It is a well-accepted fact that these long-term increases are related to the increase in emissions of aerosols of anthropogenic origin.

The increases in aerosol concentrations have shown to be an important factor counterbalancing the positive forcing on global warming due to the effect of increases in greenhouse gases (*Shine et al.*, 1996). Aerosols affect the earth's radiation balance in a direct way by blocking the downward penetration of the sun's energy in the short-wave region, and also indirectly, by acting as cloud condensation nuclei. The contributions to global radiative forcing from increases in sulphate aerosols is estimated by the Inter Governmental Panel on Climate Change (IPCC) to be  $-0.4 \text{ W/m}^2$  with a factor-of-two uncertainty. The magnitude of forcing due to the effect of aerosols on clouds is highly uncertain, but is also thought to be negative. In comparison, the increases of greenhouse gas concentrations since pre-industrial times have been estimated to result in a positive forcing of about  $+2.5 \text{ W/m}^2$ .

The changes in aerosol transmittance due to anthropogenic emissions have a timescale of decades, whereas the temporarily superimposed loading from volcanic eruptions shows a timescale from months to a few years; e.g., for the first 10 months after the recent eruption of Mt. Pinatubo in the Philippines (June, 1991), the average direct solar radiation measured at four sites, widely distributed in latitude, decreased by as much as 25-30% (*Dutton and Christy*, 1992). Another recent volcanic eruption, by Mt. El Chichon in Mexico (April 1982), had similar impacts on direct radiation, and the associated high values of aerosol optical thickness continued for 3-4 years after the eruption.

Variations of atmospheric transparency can also be superimposed on variations of solar activity, both affecting the variability of solar energy falling on the earth's surface under clear skies. Estimates of the average value of the solar constant vary slightly, depending on the estimation method used; here we have adopted a mean value of  $1367 \text{ Wm}^{-2}$ , reported to have an uncertainty of about  $\pm 0.3\%$  (*WMO*, 1986; *Lenoble*, 1993). Short-term variations of the solar constant, e.g. due to variations in the number of dark sunspots, are likely to fall within these uncertainty limits. In the long term, a slight increase in solar brightness, equivalent to a radiative forcing in the range from  $+0.1$  to  $+0.5 \text{ W/m}^2$  since the middle of the 19th century has been reported (*Shine et al.*, 1996) – an order of magnitude comparable to that estimated for aerosols.

To alleviate the large uncertainty pertaining to the role of aerosols in climate change, realistic estimates of both past as well as the anticipated future changes in aerosol concentrations are required. Monitoring programs should yield long-term trends and have global coverage, and since aerosols have a relatively short turn-over rate in the atmosphere high regional accuracy is also required. A global coverage of atmospheric transparency is best obtained from polar orbiting satellites. The archiving of weekly composite contour maps of aerosol optical thickness over the oceans from NOAA-AVHRR have been carried out since 1990 (*Stowe*, 1991). The measurements, however, are restricted to ocean areas, and retrieval methods for aerosol optical thickness still need refinements in order to obtain a match with ground-based sun photometer measurements (*Ignatov et al.*, 1995). In addition, the time series from

satellite-based observations are still too short to reveal significant trends in aerosol optical thickness. For continental areas, related satellite-based methods have been tested over inland water bodies, such as the Baltic Sea, with finer spatial resolution (Laine, 1992).

Point estimates made with ground-based radiometers provide the best long-term time series of total aerosol optical thickness over land areas. The earliest measurements, mainly from the first half of the present century, are mostly contaminated by sensor drifts and inaccurate calibration, but some good quality series begin from the 1950's. Ångström's turbidity method (Ångström, 1924) can be used to crudely estimate the size distribution of aerosols.

For the present study, short-wave broad-band measurements of the direct beam, global and diffuse radiation were available, yielding estimates of the integrated effect of all types of aerosols. Two independent methods were tested and compared to assess long-term variation of total aerosol transmittance. The first method applied an inversion of a well-established radiation transfer scheme originally developed by Bird and Hulstrom (1981) for the calculation of aerosol transmittance. The second method was based on Bouquer's principle (Kondratyev, 1969), and yielded estimates of an integrated atmospheric transparency coefficient sensitive to both aerosols and water vapour.

Data from selected sites, for which long-term daily measurements of direct beam, global and diffuse irradiance were available, were used to evaluate regional variability and detect possible erroneous anomalies in the data. The monitoring sites were Jokioinen, Jyväskylä and Sodankylä in Finland, Tiirikoja in Estonia and Bergen in Norway, all located in Northern Europe. The Sodankylä and Bergen sites represented locations far from extensive man-made combustion, while Jokioinen and Tiirikoja represented areas in the vicinity (but not under the immediate local influence) of industrial centres.

## 2. Theory

### *Determination of aerosol transmittance*

The solar irradiance under clear skies depends on the elevation angle of the sun, the solar constant and the total extinction of the atmosphere. The elevation angle of the sun is a function of time and latitude and can be accurately calculated using geometry (see Appendix). For the calculation of the global solar and diffuse irradiance at the earth's surface under clear skies, the best broad-band algorithms parameterised from detailed spectral radiation transfer schemes give root-mean-square errors close to the instrumental random error (Gueymard, 1993); e.g. Choudhury (1982) and Savijärvi (1989) have reported local accuracies of the order of 2% ( $8\text{-}16\text{W/m}^2$ ) for calculated clear sky daily integrals of global solar irradiance. However, as noted by Gueymard, the accuracy of any such scheme rests on the quality of estimates of atmospheric

turbidity and the level of accuracy to which especially the water vapour absorption and scattering/absorption by aerosols is parameterised. One of the best-performing broad-band schemes, according to tests by *Gueymard* (1993), was originally developed and tested by *Bird and Hulstrom* (1981) and later demonstrated by *Iqbal* (1983). This scheme, further referred to as IQC, makes a realistic, physically-based, estimate of the radiative effects of different absorbing and scattering media. In IQC, as well as in most of the other schemes, the integral effect of the constituents affecting atmospheric transmittance is assumed to be multiplicative, i.e., for the normal direct irradiance  $R_{dir}$  we can write

$$R_{dir} = 0.9751R_o \tau_R \tau_g \tau_w \tau_a \tau_o \quad (1)$$

where  $R_o$  is the solar constant (at a given distance from the sun) and the constant 0.9751 is included because the spectral interval considered is 0.3-3.0  $\mu\text{m}$ . The transmittance of the earth's cloud-free atmosphere primarily depends on the scattering and absorption by aerosols ( $\tau_a$ ), gaseous Rayleigh scattering ( $\tau_R$ ), absorption by ozone ( $\tau_o$ ) and absorption by water vapour ( $\tau_w$ ), and absorption by uniformly mixed gases ( $\tau_g$ ) occurring along an optical airmass  $m$ . The parameterisation of the transmittances  $\tau_R$ ,  $\tau_o$ ,  $\tau_w$  and  $\tau_g$  in broad-band schemes appears as simplified functions regressed on the results from rigorous spectral models such as SOLTRAN or LOWTRAN: details of the functions are given in *Iqbal* (1983). Least information is usually available on the aerosol transmittance  $\tau_a$ , unless dual-band irradiance data are available for the direct calculation of  $\tau_a$  by using Ångström's turbidity formula. Even with the lack of such data, also the broad-band direct-beam irradiance from the inversion of Eq. (1) (or equivalent expressions for  $R_{dir}$ ) has also been successfully used (e.g., *Unsworth and Monteith*, 1972; *Freund*, 1982; *McGuffie et al.*, 1985). When inverting Eq. (1) we obtain

$$\tau_a = R_{dir} / (0.9751R_o \tau_R \tau_g \tau_w \tau_o) \quad (2)$$

The direct normal irradiance  $R_{dir}$  can be measured directly with a (tracking) pyrheliometer; alternatively its vertical component, the direct perpendicular irradiance  $R_{dir}' = R_{dir} \sin H$ , where  $H$  is the sun's elevation angle above the horizon, can be estimated with somewhat lower accuracy from the difference of the global radiation  $R_g$  and the diffuse radiation  $R_{dif}$ , viz.  $R_{dir}' = (R_g - R_{dif})$ . Calibrated and carefully maintained measurements of  $R_g$  and  $R_{dif}$  are usually available from a few meteorological observatories in every country and thus provide a potentially valuable data source for estimating atmospheric transparency.

*Sensitivity of the components of short-wave irradiance to changes in aerosol transmittance*

Aerosols cause strong forward scattering and, to a lesser degree, absorption of the direct beam radiation energy along the path of sun's rays through the atmosphere. The fraction of energy removed from the incident beam appearing as scattered (diffuse) irradiance is called the single scattering albedo. The single scattering albedo is very close to one ( $\approx 1$ ) in the visible band of the solar spectrum for sulphate aerosols and for aerosols of oceanic origin (*d'Almeida et al.*, 1991). For shoot, dust like and water soluble aerosols the role of absorption is more pronounced and the single scattering albedo correspondingly less than one. Since aerosols affect both direct and diffuse irradiance, it is instructive to estimate, how the components of global irradiance change due to an aerosol induced change in the extinction of the atmosphere. Following the formulation in IQC we have for global irradiance

$$\begin{aligned}
 R_g &= R_{dir} \sin H + R_{dif} \\
 &= (R_{dir} \sin H + R_{dr} + R_{da}) \left( \frac{1}{1 - \alpha_s \alpha_a} \right)
 \end{aligned}
 \tag{3}$$

where  $R_{dr}$  is the diffuse irradiance because of Rayleigh scattering and  $R_{da}$  is the diffuse irradiance due to the scattering of aerosols. Multiple reflections between the earth's surface and the lower atmosphere are accounted for by the two albedos: the surface albedo  $\alpha_s$  and the albedo of the clear sky  $\alpha_a$ . The parameterisation of the components of diffuse irradiances is summarised in the Appendix.

To obtain the components of global radiation, IQC was used at two aerosol transmissivities  $\tau_a = 0.9$  and  $0.8$  with the atmospheric optical properties otherwise fixed. The results are summarised in Table 1.

From Table 1 one can conclude that for the given increase in atmospheric turbidity the increase in the aerosol diffuse scattered component  $R_{da}$ , as simulated by IQC, contributes most to the increase in the total diffuse irradiance, with an additional minor positive contribution from the enhanced multiple scattering. The direct perpendicular irradiance  $R_{dir}$  is attenuated somewhat more than the diffuse irradiance is enhanced; the resulting reduction in global irradiance due to the increase in turbidity is relatively small compared to the changes in the diffuse and direct irradiance components.

Table 1. Relative and absolute changes of the solar irradiance components at the earth's surface for an arbitrary change of atmospheric aerosol transmittance from 0.8 to 0.7, estimated by using Iqbal's broadband radiation scheme. Other parameters were kept constant and were assigned the following values (for explanation of symbols see the notation list):  $m_a = 1.919$ ,  $dc = -20.05$ ,  $F_c = 0.84$ ,  $R_o/R_o' = 1.03$ ,  $\alpha_s = 0.2$ ,  $\alpha_a = 0.08$ ,  $\omega_o = 0.9$ ,  $\tau_R \tau_o \tau_g \tau_w = 0.73$ .

Irradiance component	Mean W/m <sup>2</sup>	Absolute change W/m <sup>2</sup>	Relative change %
Diffuse aerosol scattered, $R_{da}$	59.1	+39.4	+66.7
Diffuse Rayleigh scattered, $R_{dr}$	27.1	-0.3	-1.1
Diffuse multiple scattered, $R_{dm}$	9.2	+1.4	+14.7
Total diffuse, $R_{dif}$	95.4	+40.5	+42.4
Direct normal, $R_{dir}$	828.7	-97.5	-11.8
Direct perpendicular, $R_{dir}'$	414.3	-48.7	-11.8
Global, $R_g$	509.7	-8.3	-1.6

The example also demonstrates that, for the estimation of  $\tau_a$  from surface radiation measurements, the best accuracy is obtained when the direct normal irradiance is measured directly with a pyrheliometer. When only pyranometer data on  $R_g$  and  $R_{dif}$  are available, the response to changes in  $\tau_a$  is predominately mediated through the measurement of  $R_{dif}$  which is sensitive to the correction used for the shadowing ring. *Freund* (1983) has further noted that instruments used either directly (e.g. pyrheliometer) or indirectly (e.g. two pyranometers one of which having a shadowing ring) to estimate direct solar irradiance normally have a larger effective angle of view ( $\approx 5^\circ$ ) than the angle subtended by the solar disk ( $0.5^\circ$ ); a surplus of circumsolar radiation is therefore measured as direct, rather than diffuse solar irradiance. Since the solar beam is both absorbed and strongly forward scattered by aerosols, the inclusion of some of the diffuse component in the direct radiation measurements results in a systematic underestimation of  $\tau_a$ , unless appropriate corrections are applied.

To justify the use of routine pyranometer data, emphasis was made here on the detection of relative long-term mean changes in atmospheric turbidity rather than trying to accurately assess its absolute value or local short-term variation. The pyranometers were carefully maintained, calibrated and subjected to intercomparison at the meteorological observatories; particularly it was assumed that the difference  $R_g - R_{dif}$  was insensitive to changes in the radiation environment possibly caused, e.g. by growth or removal of vegetation surrounding the pyranometer site. Conclusions on mean changes in  $\tau_a$  could also better be drawn when relatively closely-located sites were compared.

### *Atmospheric integral transparency coefficient*

The results for atmospheric aerosol transmittance obtained with the inversion of IQC were further compared with the Atmospheric Integral Transparency Coefficient AITC introduced by *Kondratyev* (1969). AITC ( $p_m$ ) is calculated from the ratio of the measured direct solar beam intensity  $R_{dir}(m)$  at the bottom of the atmosphere to the estimated intensity at the top of the atmosphere  $R_o$ . Following Bouguer's law the coefficient of transparency is then calculated from

$$p_m = \left( \frac{R_{dir}(m)}{R_o} \right)^{\frac{1}{m}} \quad (4)$$

where  $m$  is the optical air mass along the sun's rays through the atmosphere. The beam intensities  $R_{dir}(m)$  and  $R_o$  correspond to the broad band integral solar spectrum. To compare measurements made at varying sun's elevation angles,  $p_m$  is usually normalised to air mass  $m=2$  (solar elevation  $H=30^\circ$ ) to make account of the selective spectral attenuation direct beam irradiance in the atmosphere. Our comparisons of two recent normalisation procedures by *Yevnevich* and *Savikovskij* (1989) and by *Mürk* and *Ohvril* (1988, 1990) have demonstrated that both procedures give almost the same accuracy (about 2%) and that the procedures are compatible. In this investigation the latter was used yielding

$$p_2 = p_m \left( \frac{2}{m} \right)^{\frac{\log p_m + 0.009}{\log m - 1.848}} \quad (5)$$

Note the difference between the schemes for the two transmittance variables defined here: the IQC explicitly takes into account the effects of Rayleigh scattering, molecular absorption, and absorption by water vapour and ozone on the total optical transmittance, leaving the aerosol transmittance  $\tau_a$  sensitive mainly to integrated aerosol concentration. On the other hand, the AITC ( $p_2$ ) is sensitive to all constituents causing extinction of solar radiation. The effects of other constituents than aerosol, and particularly water vapour, can certainly be of importance when the causes for short-term transmittance fluctuations are being traced. However, in the long-term, average atmospheric concentrations of water vapour have been shown to be more conservative than the concentrations of aerosols, thus allowing the use of either method to monitor the effects of mean aerosol concentration changes on atmospheric transparency.

### 3. Material

The analysis employed data from five meteorological stations and observatories located in Northern Europe: Jokioinen (60°49'N, 23°30'E), Jyväskylä (62°24'N, 25°41'E) and Sodankylä (67°22'N, 26°39'E) in Finland, Bergen (60°24'N, 5°19'E) in Norway and Tiirikoja (58°52'N, 26°58'E) in Estonia. The three Finnish sites were used to demonstrate the inversion of IQC, yielding aerosol transmittance, with the direct solar beam estimated from pyranometer measurements. The AITC was calculated for four sites: Jokioinen, Sodankylä, Tiirikoja and Bergen. For these stations direct solar beam data was obtained either with pyranometers (Bergen) or with pyrhemometers/actinometers. Table 2 summarises the information related to radiation measurements made at each station.

Table 2. Information of sites and measured data.

Site	Location		Periods covered		Instrument types	
	Lat. N	Lon. E	AITC	$\tau_a$	Pyranometer	Pyrheliometer
Bergen	60°24'	05°19'	1965-1994	-	Eppley PSP	-
Jokioinen	60°49'	23°30'	1967-1991	1971-1990	Kipp&Zonen	Ångström <sup>1)</sup>
Jyväskylä	62°25'	25°40'		1971-1990	Kipp&Zonen	
Sodankylä	67°22'	26°39'	1967-1991	1971-1990	Kipp&Zonen	Silver disk, Ångström <sup>1)</sup>
Tiirikoja	58°52'	26°58'	1956-1994	-	-	AT50 Actinometer <sup>2)</sup>

1) operated manually, 2) operated with a sun tracker

Data from the Finnish stations of Jokioinen, Jyväskylä and Sodankylä consisted of both pyranometer and pyrhemometer measurements made with Kipp & Zonen instruments (models CM5 and CM11). Pyranometers were ventilated from outside to prevent formation of frost and dew. All data obtained with pyranometers were adjusted to the present international WRR scale (WMO, 1986). Diffuse radiation was measured at the Finnish sites by shading one pyranometer with a ring 60 mm in width and 240 mm in diameter. Because of the shadowing ring, the measured diffuse irradiance values were corrected upwards. The calibrations for the shadowing ring were made under near clear sky conditions with a small shading disk placed to block the sun (but not the rest of the sky). Site-specific long-term mean values of the correction multipliers were 1.15 for Jokioinen, 1.16 for Jyväskylä and 1.25 for Sodankylä for the three summer months (May, June and July) considered here. These values also correspond to operational corrections calculated by *Drummond's* (1956) method.

Direct solar beam irradiances were measured predominantly by manual orientation of the pyrhemometer towards the sun. At Tiirikoja only, automatic tracking of the sun was periodically employed. The Ångström compensation pyrhemometer was



used at the Jokioinen and Sodankylä sites for most of the time, but was temporarily replaced at Sodankylä with the Smithsonian Institute silver disk pyrheliometer. These instruments were periodically calibrated against a national standard. Repeated samples were taken around noon under (near) clear-sky conditions. A model AT50 actinometer was used at the Tiirikoja site. Data from Bergen consisted of values of  $R_{dir}$  calculated as the differences of global and diffuse solar irradiances obtained with pyranometers as documented in *Olseth and Skartveit (1989)*.

The inversion of IQC to obtain  $\tau_a$  was applied for the three Finnish sites on all qualifying hourly measurements ending at synoptic hours available since 1971 in the data base. Selection criteria were defined to limit the data to clear sky conditions (cloud coverage  $\leq 1$  octas) and given times of day (sun's elevation angle above  $10^\circ$ ) only. Winter-time (November-February) estimates were relatively scarce due to the more frequent occurrence of clouds and predominately too low a solar elevation at the latitudes considered. The dependence of calculated  $\tau_a$  on solar elevation was accounted for by an empirical fit to transmittances plotted against solar elevation angle. Using the best fit curve, instantaneous daytime hourly mean values of  $\tau_a$  were normalised to a fixed elevation of 50 degrees (the procedure is explained in detail in *Venäläinen and Heikinheimo, 1997*) representing average mid summer conditions around noon at the latitudes considered. Transmittances were further averaged over the days and months for which qualifying data existed. A monthly mean value was calculated if there were at least three daily values available for that month.

#### 4. Results

##### *Variations in atmospheric transmittance and AITC*

###### Seasonal variation

The seasonal courses of the distributions of monthly values of  $\tau_a$  and AITC were quite similar in pattern at all sites with the least seasonal variation at Bergen, Figs. 1 and 2. The lowest transparencies were reached towards the end of the summer, mainly in August, while the highest values occurred during late autumn. Also notable is the increase in transparency with latitude, as the highest transparencies occurred on average at Sodankylä, the northernmost site, and lowest values at Tiirikoja, the southern most site. For comparison, *Freund (1983)*, reports an opposite pattern for transparency in the Northern American high-latitude Arctic zone: a spring minimum and summer maximum.

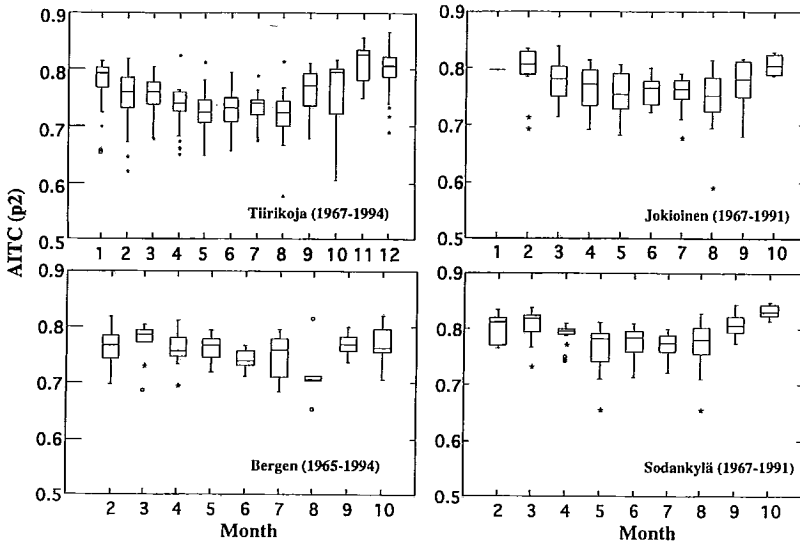


Fig. 1. Seasonal course of mean monthly AITC ( $p_2$ ) expressed as distributions over the period from 1965 to 1994 at the Sodankylä, Jokioinen, Tiirikoja and Bergen sites. The horizontal line within the box corresponds to the median, the hinges of the box to an interquartile range, and the whiskers to a  $\pm 1.5$  times the interquartile range of monthly mean values. Symbols \* and o denote exceptional anomalous values.

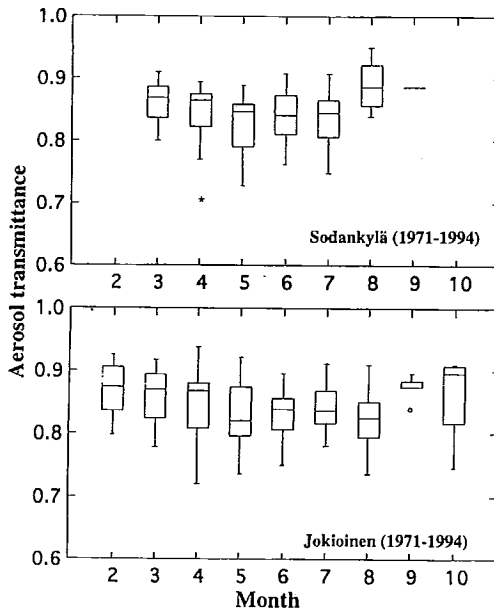


Fig. 2. Same as Fig. 1, but for the aerosol transmittance  $\tau_a$  and the Sodankylä and Jokioinen sites.

### Long-term year-to-year variation

The time variation of monthly mean aerosol transmittances  $\tau_a$ , obtained with the IQC, for the three Finnish sites is shown in Fig. 3. The figure presents the year-to-year variation of the mean monthly normalised aerosol transmittance from 1971 to 1994 at the Jokioinen, Jyväskylä, and Sodankylä observation stations. This is an update of the previous analysis by *Laine* (1992) based on data from five sites in Finland, but for the period from 1971 to 1990. The correspondence of the time series between the three stations shown here and the two additional sites shown by Laine was good. The gaps in the data mainly correspond to the winter months (November-January), for which the estimates of transmittance were omitted due to low accuracy and the scarce occurrence of qualifying conditions. The low-pass filtered variation of aerosol transmittance was exhibited by using a twelve month moving average which smoothes out most of the seasonal variability. The aerosol transmittance was related to aerosol optical thickness (or depth)  $\delta_a$  using the relation

$$\delta_a = -\ln \tau_a \quad (6)$$

Since  $\tau_a$  was normalised to an elevation angle of  $50^\circ$ , the scale for  $\delta_a$  in Fig. 3 correspond to an optical mass of  $m \approx 1.3$ .

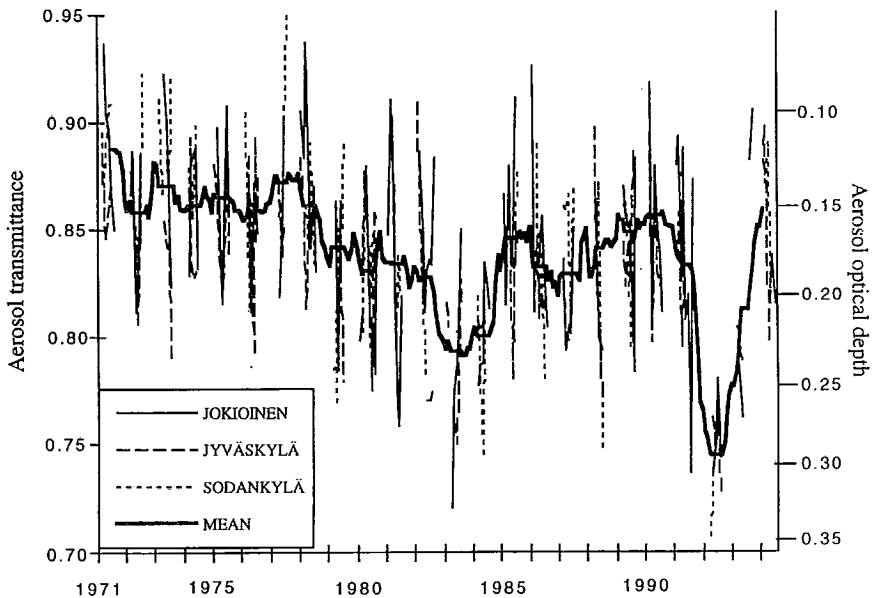


Fig. 3. Year-to-year variation of the mean monthly normalised aerosol transmittance  $\tau_a$  from 1971 to 1994 at the Jokioinen, Jyväskylä, Sodankylä sites (Finland). Data from winter months is not included. The solid line corresponds to a 12-month moving average calculated from the monthly means for all three sites.

The second data set consisted of a monthly mean AITC's as derived from measurements made with pyrhemometers and actinometers at Tiirikoja, Sodankylä, Jokioinen and Bergen. To compare long-term changes of transmittance between the sites for the detection of possible anthropogenic effects, the year-to-year summer time (May-July) mean values of transmittance were calculated, Fig. 4. The summer season was selected because the month-to-month change in transparency between May, June and July was relatively small compared to the monthly course of transparency for the spring or autumn seasons as seen in Figs. 1 and 2. The time series from Tiirikoja was almost complete from 1956 to 1994, for which also a series of annual mean values of AITC ( $p_2$ ) is shown in Fig. 5. Other series started from 1965 onwards with some gaps (see Table 2).

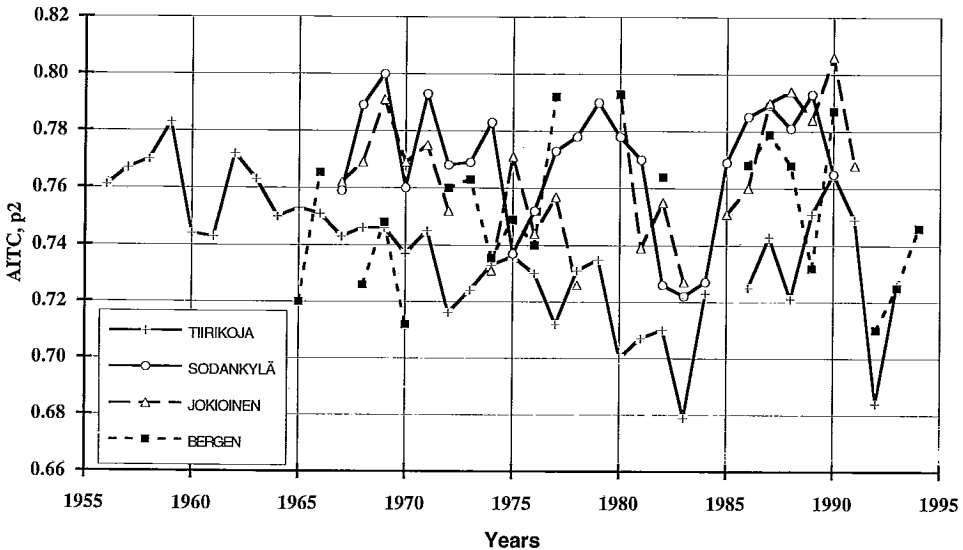


Fig. 4. Year-to-year variation of the summer time mean (May-July) AITC ( $p_2$ ) at Jokioinen and Sodankylä (Finland), Tiirikoja (Estonia) and Bergen (Norway) for the available years during the period from 1956 to 1993.

The overall trend, in Fig. 3, for smoothed values is negative of  $\tau_a$  (or positive for  $\delta_a$ ) at all Finnish sites, indicating a gradual decrease in aerosol transmittance (increase in atmospheric turbidity) since the beginning of the 1970's. A similar overall negative trend of AITC is seen in Figs. 4 and 5, and ongoing already in the 1960's. The tendency towards lower  $\tau_a$  or AITC values is most pronounced during the 1960's and the 1970's whereas the high variation caused by volcanic activity in the 1980's and early 1990's makes continuation of this negative trend during the 1980's and 1990's uncertain.

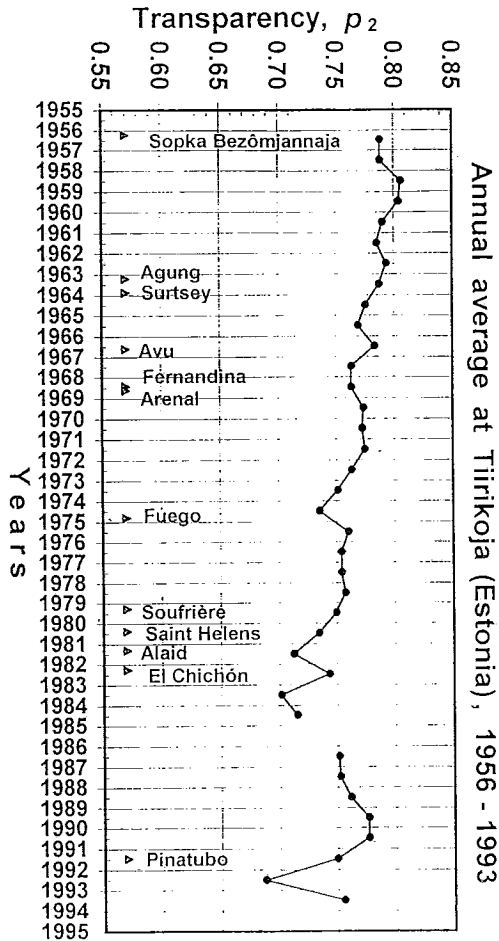


Fig. 5. Year-to-year variation of the annual average AITC ( $p_2$ ) at Tiirikoja (Estonia) for the period from 1956 to 1993.

The two temporary minima, peaking in 1983-1984 and 1992, seen on both data sets, correspond to the volcanic eruptions of El Chichon (April, 1982) and Mt. Pinatubo (June 1991). Other volcanic occurrences are also pointed to in Fig. 5, but their effects are not as pronounced. The maxima in terms of aerosol optical thickness  $\delta_a$ , of the order of +0.07 for the eruption of El Chichon and +0.15 for Mt. Pinatubo (with respect to values just preceding and following the short term anomaly, see Fig. 3), are also well in line with the anomalies of aerosol optical thickness reported by *Dutton and Christy* (1992) for stations widely distributed globally.

A comparison of the mean trends of aerosol transmittance and AITC measured at different sites was made by selecting a period from the available data visualised in Figs. 3 - 5. To exclude the effect of Mt. Pinatubo eruption, the comparison period was not extended later than 1991. The aim was to emphasise possible recent causes from the changes of anthropogenic emissions. Since the Pinatubo minimum appeared at the end of the data series this would have significantly biased the trend estimates.

The mean trends of  $\tau_a$  and AITC ( $p_2$ ), expressed as % change/decade, for the available time periods until 1991, are summarised in Tables 3 and 4 for those months for which the significance level was above 50%. All trends that were significant at 95% level were negative, confirming the visual impression from Figs. 3-5. Concluding from Table 3, mean changes of  $\tau_a$  range from -2.4 to -4.6 (% per decade) with a tendency to stronger decrease at the Sodankylä site compared to Jokioinen. Referring to Table 1, where the implications of a given change in  $\tau_a$  on the solar radiation components were estimated, an order of -3% change of  $\tau_a$  (e.g. from 0.85 to 0.82) would correspond to a reduction of global radiation of about 0.4% ( $2 \text{ W/m}^2$  for a level of  $500 \text{ W/m}^2$ ) based on IQC-scheme. In comparison, a -1% change of AITC ( $p_2$ ) would be required, based on Eq. (3), to produce a corresponding change in global radiation. Trends of AITC ( $p_2$ ) for Tiirikoja, for the period from 1956 to 1991 range from -1.5 to -2.8 (% per decade) indicating a slightly larger increase in turbidity than obtained for the Finnish sites.

In comparison to the Tiirikoja site, the AITC ( $p_2$ ) generally exhibits higher values at the three Finnish and the Bergen sites. The Finnish sites show a negative trend of AITC for the 1970's, but the available period is too short to reveal statistical significance. Correlation of these sites with the more distant Bergen site is rather weak.

Table 3. Mean trends (% per decade) of monthly mean aerosol transmittance  $\tau_a$  calculated for the three Finnish sites for the period preceding the eruption of Mt. Pinatubo from 1971 to 1991. Trends typed in bold indicate significance at 95% level.

Month	Jokioinen	Sodankylä	Jyväskylä
April	<b>-4.4</b>	0.3	-2.0
May	-0.8	-1.1	-1.3
June	<b>-2.7</b>	<b>-3.4</b>	-1.4
July	<b>-2.4</b>	<b>-4.6</b>	<b>-3.7</b>
August	<b>-4.0</b>	-4.5	1.8
September	2.7		-5.1

Table 4. Mean trends (% per decade) of monthly mean AITC ( $p_2$ ) at Tiirikoja, Estonia for the period preceding the eruption of Mt. Pinatubo from 1971 to 1991. Trends typed in bold indicate significance at 95% level.

Month	Tiirikoja
January	<b>-1.7</b>
February	<b>-1.9</b>
March	<b>-1.5</b>
April	<b>-1.8</b>
May	-1.0
June	<b>-1.1</b>
July	<b>-0.9</b>
August	<b>-1.7</b>
September	-0.7
October	<b>-2.8</b>
November	-0.1
December	<b>-1.8</b>
Annual mean	<b>-1.4</b>

### 5. Summary and discussion

Atmospheric transmittance has been expressed either as an aerosol transmittance  $\tau_a$  obtained by inversion of a well-established broad-band radiation transfer scheme, or as an atmospheric integral transparency coefficient AITC ( $p_2$ ). The transmittance  $\tau_a$  was expected to be rather insensitive to variations in the total water vapour content, whereas  $p_2$  responded to all factors affecting turbidity along an atmospheric optical path normalised to  $m=2$ . The relative variation of the transmittance parameters was emphasised here, as known sources of error may possibly cause systematic bias in the absolute level of transmittances  $\tau_a$  and AITC ( $p_2$ ). Random variability (i.e. noise) was small enough to obtain correspondence of data series between closely adjacent sites and a realistic response to known increases in turbidity caused by recent volcanic eruptions.

The records allowed analysis of the mean changes of atmospheric turbidity for the past 3-4 decades at the selected sites in Northern Europe. At all sites, except Bergen, the turbidity had increased (transmittance decreased) during the 1960's and 1970's, but the sign of the trend from the 1980's onwards was uncertain due to the overlap of the effect of volcanic eruptions of El Chichon and Mt. Pinatubo with the long-term mean change of transparency. The negative trend in turbidity for the period from the 1960's to the 1980's was most notable in the long time series of annual mean AITC from Tiirikoja starting from 1956. A corresponding decrease in global radiation is estimated to be about  $2 \text{ W/m}^2$ . Since the transparency before and after the Mt.

Pinatubo minimum in 1991-1993 was at the same level as at the end of the 1970's, it is possible that at the present time the drop in atmospheric transparency in this region has ceased and may even have obtained an increasing trend.

The seasonal patterns of  $\tau_a$  and  $p_2$  were quite similar both at Jokioinen and Sodankylä, for which both variables were calculated; the seasonal courses indicated a summer minimum and late autumn maximum for transparency. This indicated that the seasonal course of the water vapour content of the atmosphere, having a minimum in winter and a maximum in summer, could have contributed to the seasonal course of both  $\tau_a$  and  $p_2$ . Since the effect of variations of atmospheric precipitable water in  $\tau_a$  are accounted for through the transmissivity  $\tau_w$  in IQC, it is likely that the parameterisation does not account for all the effects, and particularly for the interaction of aerosols and water vapour on turbidity. No significant long-term trend was detected in the precipitable water content during the period considered; the observed variation of transmissivity could therefore be mainly assigned to the effects of aerosols.

The results indicated that routine monitoring of solar radiation with the standard set of pyranometers measuring global and diffuse short-wave solar radiation and the application of a physically-based radiation transfer scheme can produce long-term time series of atmospheric aerosol transparency. This method, although yielding rather crude estimates, is particularly valuable in analysing past changes of atmospheric transparency for which no satellite data exists and where networks of sites measuring direct beam irradiance with pyrheliometers have been sparse. The relative variation of transparency seems to be well detected with both methods presented here; however, further careful comparisons, e.g., with dual-band sun photometer measurements, should be made. These comparisons could detect systematic errors possibly introduced by the seasonal or year-to-year variation in the size/type distribution of aerosols.

A significant portion of atmospheric aerosol is formed when certain gases, such as sulphur dioxide and nitrous oxide are emitted, mostly due to anthropogenic activity, into the atmosphere. Long-term mean changes in atmospheric transparency may therefore be traced to changes in industrialisation and to the development of techniques for the prevention of air pollution. Long-term monitoring of air quality at several surface sites in Finland has revealed an improving trend since the start of the present programme in 1980 (Leinonen, 1996). This is particularly demonstrated as a gradual drop in the annual means of aerosol sulphate concentrations and depositions from 1980 to 1994. The corresponding annual nitrate deposition has also decreased at many locations. One could therefore speculate that the levelling-off of atmospheric transparency in this corner of Northern Europe is most likely caused by improvements in the prevention of anthropogenic sulphur and nitrous compound emissions.

#### *Acknowledgements*

The authors are indebted to all the technicians at the observation sites whose long-term contribution made this analysis possible. We particularly thank Mr. Asko



Tuominen and Ms. Leila Laitinen of FMI for making available the Finnish data. The work was partially supported by the Finnish Research Programme of Climate Change SILMU through the Academy of Finland.

## 6. References

- d'Almeida, P. Koepke and E.P. Shettle, 1991. Atmospheric Aerosols: Global Climatology and Radiative Characteristics. Deepak Publishing, Hampton Virginia USA, 559 pp.
- Ball, R.J. and G.D. Robinson, 1982. The origin of haze in the Central United states and its effects on solar radiation. *J. Appl. Meteor.*, **21**, 171-188.
- Bird, R. and R.L. Hulstrom, 1981. Direct insolation models. *Trans. ASME Journal of Solar Energy Engineering*, **103**, 182-192.
- Choudhury, B., 1982. A Parameterised model for global insolation under partially cloudy skies. *Solar Energy*, **29**, 479-486.
- Drummond, A.J., 1956. On the measurement of Sky radiation. *Arch. Met. Geophys. Biokl. Serie B*, **7**, 413.
- Dutton, E.G. and J.R. Christy, 1992. Solar radiative forcing at selected locations and evidence for global lower tropospheric cooling following the eruptions of El Chichon and Pinatubo., *Geoph. Res. Lett.*, **19**, 2313-2316.
- Freund, J., 1983. Aerosol optical thickness in the Canadian Arctic. *Atmosphere-Ocean*, **21**, 158-167.
- Gueymard, C., 1993. Critical analysis and performance assessment of clear sky solar irradiance models using theoretical and measured data. *Solar Energy*, **51**, 121-138.
- Ignatov, A., L. Stowe, R. Singh, S. Sakerin, D. Kabanov and I. Dergileva, 1995. Validation of NOAA/AVHRR Aerosol retrievals using the sun-photometer measurements from R/V Akademik Vernadsky in 1991. *Advances in Space Research (COSPAR 1996)*, **16**, (10)95-(10)98.
- Iqbal, M., 1983. *An Introduction to Solar Radiation*. Academic Press Canada, Ontario. 390 p.
- Kondratyev, K.Ya., 1969. *Radiation in the atmosphere*. Academic Press, New York, 912 p.
- Laine, V., 1992. Atmospheric aerosol optical thickness and size distribution from satellite data over the Baltic Sea. *Comm. Phys. Math. et Chem Med*, 137/1992, Finnish Soc. Science and Letters, Acad. Dissert., pp. 93.
- Leinonen, L (Ed.), 1996. *Ilmanlaatumittauksia - Air quality measurements*. Finnish Meteorological Institute. Helsinki, 235 pp.
- Lenoble, J., 1993. *Atmospheric radiative transfer*. A. Deepak Publishing, Hamton, Virginia, U.S.A., 241-242.

- McGuffie, K., J.G. Cogley and A. Hendersson-Sellers, 1985. Climatological analysis of arctic aerosol quantity and optical properties at Resolute, N.W.T.. *Atmospheric Environment*, **19**, 707-714.
- Mürk, H. and H. Ohvril, H. 1988. The formula to convert the integral transparency of the atmosphere to relative optical mass  $m=2$  and to arbitrary mass  $M$ . *Proc. all-union seminar on the numerical methods in solving the transport equation*. Ac.Sc.ESSR, Tartu, Estonia, 138-141 (in Russian).
- Mürk, H. and H. Ohvril, H. 1990. Engineer method to convert the transparency coefficient of the atmosphere from one relative optical mass to another. *USSR Meteorology and Hydrology*, **1**:103-107, (In Russian).
- Olseth, J.A. and A. Skartveit, 1989. Observed and modelled hourly luminous efficacies under arbitrary cloudiness, *Solar Energy*, **42**, 221-233.
- Radionov, V.F. and M.S. Marshunova, 1992. Long-term variations in the turbidity of the arctic atmosphere in Russia., *Atmosphere-Ocean*, **30**, 531-549.
- Russak, V., 1990. Trends of solar radiation, cloudiness and atmospheric transparency during recent decades in Estonia. *Tellus*, **42B**, 206-210.
- Savijärvi, H., 1989. Fast radiation parameterization schemes for mesoscale and short-range forecast models. *J. Appl. Meteor.*, **29**, 437-447
- Shine, K.P., Y. Fouquart, V. Ramaswamy, S. Solomon and J. Srinivasan, 1996. Radiative forcing. IPCC -XI/Doc 3 (II).
- Stowe, L., 1991. Cloud and aerosol products at NOAA/NESDIS, *Paleogeogr. Paleoclim. Paleoecol.*, **90**, 25-32.
- Unsworth, M.H. and J.M. Monteith, 1972. Aerosol and solar radiation in Britain. *Q.J.R. Met. Soc.*, **98**, 778-797.
- Venäläinen, A., and M.J. Heikinheimo, 1997. The spatial variation of long-term mean global radiation in Finland. To appear in *Int. Journal of Climatology*.
- Yevnevich, T.V. and I.A. Savikovskij, 1989. Calculation of direct solar radiation and of the coefficient of atmospheric transparency. *USSR Meteorology and Hydrology*, **5**, 106-109 (In Russian).
- WMO, 1986. Revised instruction manual on radiation instruments and measurements. WCRP Publication series No. 7, WMO/TD-No.149, World Meteorological Organization, Geneva. pp. 140.
- Ångström, A. 1924. Report to the international commission for solar research on actinometric investigations of solar and atmospheric radiation. *Quart. J. Roy. Met. Soc.*, **50**, p. 121.

## APPENDIX

This section summarises the equations and methods used to calculate the solar constant at the top, and the diffuse of solar irradiance at the bottom, of the atmosphere. The method follows that presented by *Iqbal* (1983). References to original sources are omitted for brevity. For the calculation of transmittances due to ozone absorption  $\tau_o$ , Rayleigh scattering  $\tau_R$ , gaseous absorption  $\tau_g$ , and water vapour absorption  $\tau_w$ , see also *Iqbal* (1983).

### *Geometric equations*

The systematic fluctuation of the solar constant  $R_o$  (in  $W/m^2$ ) on a surface normal to the sun's beam at the top of the atmosphere, due to the sun's excentricity, can be calculated from

$$R_o = R_o' (1.000110 + 0.034221 \cos \Theta + 0.001280 \sin \Theta + 0.000719 \cos 2\Theta + 0.000077 \sin 2\Theta) \quad (A1)$$

where  $R_o'$  ( $=1367 W/m^2$ ) is the solar constant at mean distance from the sun,  $\Theta = 2\pi(d-1)/365$  is the day angle (in radians) and  $d$  is the running date from 1 January. The sine of the sun's elevation angle  $H$  is given as

$$\sin H = \cos(\varphi) \cos(dc) \cos[(t-12)2\pi/24] + \sin(\varphi) \sin(dc) \quad (A2)$$

where  $\varphi$  is the latitude and  $t$  the local solar hour. The declination angle ( $dc$ ) can be obtained from

$$dc = (0.006918 - 0.399912 \cos \Theta + 0.070257 \sin \Theta - 0.006758 \cos 2\Theta + 0.000907 \sin 2\Theta - 0.002697 \cos 3\Theta + 0.00148 \sin 3\Theta)(180/\pi) \quad (A3)$$

### *Components of diffuse irradiance*

The Rayleigh scattered irradiance after the first pass through the atmosphere is

$$R_{dr} = 0.79 R_o \sin H \tau_o \tau_g \tau_w \tau_{aa} 0.5(1 - \tau_R) / (1 - m_a + m_a^{1.02}) \quad (A4)$$

where  $m_a$  is the relative optical mass and the transmittance of direct radiation due to aerosol absorptance  $\tau_{aa}$  is expressed ( $\omega_o \approx 0.6-0.9$  is the single scattering albedo) as

$$\tau_{aa} = 1 - (1 - \omega_o)(1 - m_a + m_a^{1.06})(1 - \tau_a) \quad (A5)$$

The aerosol-scattered diffuse irradiance after the first pass through the atmosphere

$$R_{da} = 0.79R_o \sin H \tau_o \tau_g \tau_w \tau_{aa} F_c (1 - \tau_{as}) / (1 - m_a + m_a^{1.02}) \quad (\text{A6})$$

where  $F_c$  is the fraction of forward scattering to total scattering ( $\approx 0.8$ ) due to aerosols and  $\tau_{as}$  is the transmittance due to scattering by aerosol and is defined as

$$\tau_{as} = \tau_a / \tau_{aa} \quad (\text{A7})$$

Multiple reflections between the ground surface and the atmosphere result in an additional diffuse component  $R_{dm}$  written as

$$R_{dm} = (R_{dir} \sin H + R_{dr} + R_{da}) \alpha_s \alpha_a / (1 - \alpha_s \alpha_a) \quad (\text{A8})$$

where the expression used for clear -sky albedo reads

$$\alpha_a = 0.0685 + (1 - F_c)(1 - \tau_{as}) \quad (\text{A9})$$

The total diffuse radiance can be finally calculated from the sum of components as

$$R_{dif} = R_{dr} + R_{da} + R_{dm} \quad (\text{A10})$$

## NOTATION

$d$	running date from 1st January
$dc$	declination angle (radians)
$F_c$	fraction of forward scattering to total scattering due to aerosols, $\approx 0.8$
$H$	sun's elevation angle (radians)
$m$	optical mass
$m_a$	relative optical mass, optical mass at local pressure
$p_m$	transparency coefficient AITC
$R_{da}$	diffuse irradiance produced by aerosol scattering ( $\text{W/m}^2$ )
$R_{dm}$	diffuse irradiance produced by multiple reflections between the atmosphere and the ground surface ( $\text{W/m}^2$ )
$R_{dif}$	total diffuse irradiance on a horizontal surface ( $\text{W/m}^2$ )
$R_{dr}$	diffuse irradiance produced by molecular scattering ( $\text{W/m}^2$ )
$R_{dir}$	direct solar beam irradiance ( $\text{W/m}^2$ )
$R_{dir}'$	component of direct solar beam irradiance normal to a horizontal surface ( $\text{W/m}^2$ )
$R_g$	total global irradiance on a horizontal surface ( $\text{W/m}^2$ )
$R_o$	solar constant ( $\text{W/m}^2$ )
$R_o'$	solar constant at mean distance from the sun ( $1367 \text{ W/m}^2$ )
$t$	local solar hour

$\alpha_a$	albedo of the clear sky
$\alpha_s$	albedo of terrain surface
$\delta_a$	aerosol optical thickness
$\varphi$	latitude (radians)
$\Theta$	running day of the year expressed in radians
$\tau_a$	transmittance produced by aerosols, aerosol transmittance (fraction of the incident energy transmitted by the aerosols)
$\tau_{aa}$	transmittance due to absorption by aerosols
$\tau_{as}$	transmittance due to scattering by aerosols
$\tau_g$	transmittance due to gaseous absorption
$\tau_o$	transmittance due to ozone absorption
$\tau_R$	transmittance due to Rayleigh scattering
$\tau_w$	transmittance due to water vapour absorption
$\omega_o$	single scattering albedo, fraction of the incident energy scattered to total attenuation by aerosols